Research Article | Vol. 28, No. 18 / 31 August 2020 / Optics Express 25716

Optics EXPRESS

# Femtosecond laser hybrid fabrication of a 3D microfluidic chip for PCR application

CHAO SHAN,[1] CHENGJUN ZHANG,[2] JIE LIANG,[1] QING YANG,[2,3] HAO BIAN,[1] JIALE YONG,[1] XUN HOU,[1] AND FENG CHEN[1,4]

[1] *State Key Laboratory for Manufacturing System Engineering and Shaanxi Key Laboratory of Photonics Technology for Information, School of Electronic Science and Engineering, Xi'an Jiaotong University, Xi'an 710049, China*
[2] *School of Mechanical Engineering, Xi'an Jiaotong University, Xi'an 710049, China*
[3] *yangqing@xjtu.edu.cn*
[4] *chenfeng@mail.xjtu.edu.cn*

**Abstract:** Microfluidic chips have gradually become a focus of scientific research. However, the fabrication of key functional components in microfluidic chips is always limited by the existing processing methods. The microfluidic chip is difficult to be three-dimensional (3D) and integrated. In response to the key problems of 3D integrated microfluidic chip fabrication, this paper presents a hybrid method for fabricating a microfluidic chip integrated 3D microchannels and metal microstructures by femtosecond laser wet etch technology and liquid metal injection. The integrated microfluidic chip fabricated by this method is expected to be applied to the core reaction unit of integrated PCR devices.



## 1. Introduction

Microfluidic chips are combination of modern biochemical detection technology and micromachining technology. Through micromachining technology, the basic structures of microchannels, micropumps, microvalves, and microelectrodes are integrated into a single micro-fluidic chip. With the miniaturization and integration of biochemical analysis equipment, the microfluidic chips can realize the functions of biological or chemical laboratories on a micrometer or millimeter scale chip. These functions include sample fabrication, reaction, separation and detection in chemical analysis; cell lysis, nucleic acid separation and detection in biological testing [1–3].

The rapid development of micromachining technology and biochemical detection technology has promoted the development of microfluidic chips. With the development of micromachining technology, the functions of microfluidic chips are becoming more and more diverse. At present, the research content of microfluidic chips mainly focuses on two aspects: micro-nano integrated fabrication process and biochemical detection technology. As an important component of microfluidic chips, key functional components such as microchannels, micromixers, microelectrodes and electromagnetic controllers are particularly important to improve the performance of microfluidic chip. Micro-nano devices with complex 3D structure can not only improve the integration degree of microfluidic chips, but also expand the application function of microfluidic chips and improve its detection performance.

However, the existing micromachining technology, such as the fabrication method based on the semiconductor lithographic plane process [4], can only produce two-dimensional or simple 3D-devices even if the most complex multi-layer mask processing is adopted. It is difficult to fabricate 3D microchannels and 3D metal micro-nano structures, and it is even more difficult to integrate the two structures. This has become a bottleneck problem in the research of 3D microfluidic machining technology. Therefore, there is an urgent to develop a new processing method for 3D integrated microfluidic chips, which can effectively improve the integration and performance of the chip. Such as compress the size of the device and reduce the distance between

#398848 https://doi.org/10.1364/OE.398848
Journal © 2020 Received 10 Jun 2020; revised 4 Aug 2020; accepted 9 Aug 2020; published 17 Aug 2020

Optics EXPRESS

each unit. The 3D integrated microfluidic chips can also improve the performance of temperature field or magnetic field generated by metal micro-nano structures to be more uniform.

In recent years, femtosecond laser technology has become one of the frontiers and hot research directions in the field of 3D micro-nano manufacturing [5–8]. Femtosecond laser micromachining has unique advantages in 3D microchannel structure and microfluidic chip fabrication, and many innovative research results have been obtained [9–14]. In the previous study [15], we used femtosecond laser wet-etching technology to fabricate complex three-dimensional microchannel structures in fused silica. On the basis of the research work, we propose a method of fabricating 3D metal microstructure by importing the metal into the prepared 3D micro-channel structure after liquefaction at high temperature, thus forming 3D metal micro-nano structures [16,17]. The fabrication of 3D microchannel structure and 3D metal microstructure provides us with the idea of fabricating and integrating the two structures on the same chip.

As the fabrication of these two structures is based on the femtosecond laser wet etching technology, the microchannel structure and metal microstructure can be arranged on the chip through an integrated design. Taking the advantage of 3D distribution, the arrangement does not merely list the two structures separately, but nest the two structures together. This design will further reduce the chip size; improve the chip integration and performance. The three-dimensional microfluidic chip enables it to have rapid heating and cooling capacity, and also improves the uniformity of the temperature field, controlling the temperature difference within 1°C. After just one step of femtosecond laser modification and wet etching, the integrated structure can be machined. This method greatly reduced the processing steps and difficulty. In this paper, we use a liquid metal called galinstan instead of the gallium metal, which is used in the previous work. Because the gallium metal is prone to fuse when high current loaded. Experimental results show that when the galinstan is heated to 100°C, the microcoil structure can still guarantee the current conduction, ensuring the stability and reliability of the chip. In addition, the galinstan also has better fluidity, can effectively solve the problem of the gallium metal blocking in the microsolidifying process. The application of galinstan improves the success rate of chip fabrication and the electrothermal performance of the chip.

The polymerase chain reaction (PCR) process is a typical biological detection technology which uses temperature field control to realize nucleic acid amplification via polymerase chain reaction. The PCR has assumed important tasks in the detection of major infectious diseases, such as SARS, Ebola and the recent outbreak of the COVID-19. To realize miniaturized and integrated PCR instrument is an important research direction of microfluidic devices fabrication [18–20]. One of the important tasks is to integrate the core units (temperature control unit and reaction unit) on the same chip. However, the fabrication of the core microchip of PCR instrument also has the problem that the 3D structure is difficult to be integrated on the same chip. Therefore, this paper proposes to fabricate an integrated microfluidic chip by femtosecond laser wet etching and liquid metal injection technology. The chip could provide accurate, stable and uniform temperature environment for the reaction unit of PCR microchip. By this approach, the integrated microfluidic chip is expected to be applied to the core unit of small integrated PCR instrument.

## 2. Experiment

The microchips include of one microcoil and several microchannels. The fabrication of microfluidic chip is an integrated and hybrid manufacturing process. The microfluidic chip manufacturing process includes two steps: production of 3D microchannels, and injection with metal galinstan into the channels in the fused silica.

The femtosecond laser micromachining system is used to fabricate the microchannels involves a femtosecond laser source (wavelength: 1030 nm, pulse duration: 130 fs, repetition rate: 10 kHz), a microscope objective (NA = 0.85, 100×), a programmable three-axis stage (H101A

Optics EXPRESS

ProScan II Upright Stage; Prior Scientific), a charge-coupled device camera, and a laser beam control system. The microchannel was fabricated embedded in the fused-silica substrate (1.0 cm × 1.0 cm × 1 mm). The channel was written by the femtosecond laser with moving the 3D stage along the pattern path at a speed of 100 μm/s. The pulse energy is 15.3 μJ and the peak power is 117.7 kW. The laser power was adjusted from 40 mW to 60 mW by a computer-controlled attenuator. The geometry of the channel, the height, and the pitch circle diameter of the helix can be controlled by computer. The sample was immersed in an ultrasound-assisted solution of 5% hydrofluoric acid (HF) for 1 hour, which is called pre-etching. Then the sample was put into another solution of 10% HF for about 2 hours, and a hollow spiral channel with a dimension of 40 μm was obtained. To create the connector for the injection process, the fused-silica sample was placed on a prepared polydimethylsiloxane (PDMS) film. Before the bonding process, the fused silica chip and the PDMS film were cleaned twice in the ethanol ultrasonic bath and dried by the nitrogen flow. The bonding surfaces of the fused silica and PDMS are treated by the oxygen plasma for 80 seconds, and then bonded them together under room temperature conditions. When the fused silica chip is in contact with the PDMS film, the bonding becomes stable by suitably extruded with hands. Two syringe needles were inserted into the PDMS film at the entrance of the channel, then, the liquid galinstan is injected at one side of the coil by a syringe pump with a low speed of 0.1 mL/h at room temperature. Meanwhile, it is sucked by a suction pump in another entrance. The galinstan metal presents full filling of the helical microchannel to achieve conductive microcoils. Thus, the entire microfluidic chip was integrated, as shown in Fig. 1.

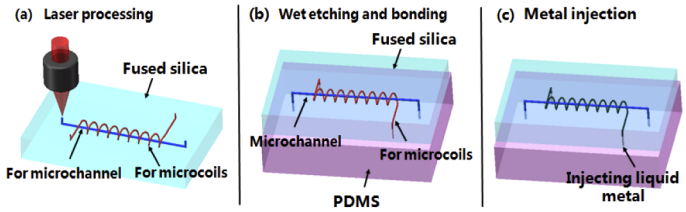


**Fig. 1.** Schematic diagram of the fabrication process.

## 3. Result and discussion

By femtosecond laser wet etching and liquid metal injection, we fabricate a simple hybrid integrated structure. It is composed of a microcoil and a straight microchannel which through from the axis direction of the microcoil, as shown in Fig. 2(a). For the helical microcoils, the number of turns, length, helical pitch, and circle diameter are 10, 2000, 200, and 200 μm, respectively. The diameter of the cross-section is 35 ± 1 μm. Using the three-dimensional properties of the structure, we successfully integrated the metal microstructure with the microchannel structure on a chip. The microchannel structure is closely surrounded by the microcoil structure with spacing less than 100 microns. This result shows that the processing method we adopted can effectively fabricate 3D micro-nano structure with high integration degree.

On this basis, we designed a more complex integration structure. This structure integrates the microcoil and three-dimensional spiral micromixer on a chip, as shown in Fig. 2(c). For the helical microchannel mixer and microcoils, the number of turns, length, helical pitch, circle diameter, and depth of the helix axis with respect to the sample surface are 8, 1600, 200, 200, and 175 μm, respectively. The diameter of the cross-section is 35 ± 1 μm. The helical structure of the micromixer and the microcoil is nested within each other. The spacing between the microchannel structure and the microcoil structure per turn is also less than 100 microns. This integrated structure can provide the required temperature for the reaction while completing the mixing

Optics EXPRESS

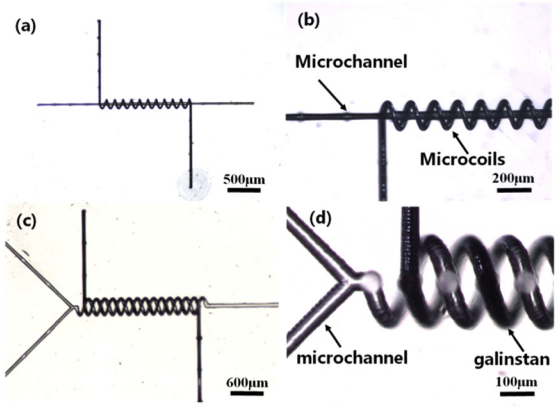


**Fig. 2.** (a) The optical microscope image of fabricated hybrid integrated structure (b) The locally enlarged image of the structure (c) The optical microscope image of fabricated true 3D PCR chip (d) The locally enlarged image of the chip.

of experimental samples. This ensures the performance of the hybrid reaction and extends the application range of the microfluidic chip.

The process of PCR is that the reactant such as nucleic acid is cycled repeatedly at three different temperatures, resulting in a large number of amplification. The designed and fabricated microfluidic chip integrated with metal microstructure and microchannel structure can provide the channel and temperature field needed for the PCR process. Therefore, in order to realize that the fabricated microfluidic chip can be applied to PCR process, we tested the temperature control performance of our chip. It mainly includes the accuracy of temperature control, the rate of heating/cooling and the cycle test of temperature field.

First, we tested the accuracy of temperature control of the microfluidic chip. This chip takes advantage of the electrothermal characteristics of the microcoils, and loads different amounts of current to make the chip reach different temperatures. The temperature of the microcoils is obtained by an infrared thermal imager (Flk-Xlens/Stan, Fluke Tix 660). We tested the chip surface temperature after 1 minute under different current loading, and the result is shown in Fig. 3(a). As can be seen from the Fig. 3(a), the surface temperature of the chip tends to be stable after a 1-minute heating process. Therefore, we call the temperature at this moment as "stable temperature". We establish a relationship curve between the loading current and the stable temperature shown in Fig. 3(b). At the same room temperature, this relationship curve can be obtained after many tests. This result shows that the precise temperature of PCR reaction can be provided by fine control of loading current.

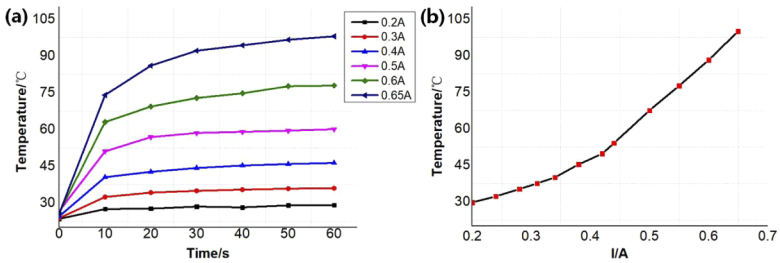


**Fig. 3.** (a) Heating properties of the microcoils at different electric currents. (b) The relationship curve between the loading current and the stable temperature.

Optics EXPRESS

We used infrared thermal imager to test the distribution of temperature field generated by microcoils, and analyzed the test results with the help of post-processing software. The results are shown in Fig. 4. The infrared real-time picture in Fig. 4(a) shows the steady-state temperature field distribution on the chip surface when the loaded current is 0.51A. The highest temperature appears at the center of the microcoil, which is 73.33°C. The uniformity of the temperature field in the 3 mm * 3 mm area around the microcoil was analyzed, and the temperature distributions of line ac and line bd were studied, as shown in Fig. 4(b). It can be seen that within the range of microcoil length direction (line ac from 1 mm to 2 mm), the highest temperature is 73.33°C, the lowest temperature is 71.6°C, and the temperature difference is 1.73°C. In the range of microcoil diameter (line bd from 1.4 mm to 1.6 mm), the maximum temperature is 73.33°C, the minimum temperature is 72.9°C, and the temperature difference is 0.43°C.

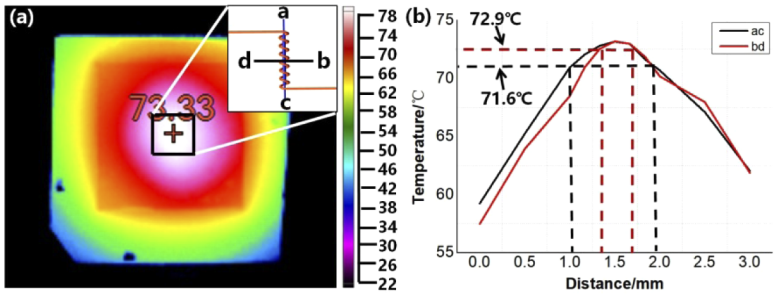


**Fig. 4.** Temperature field uniformity test results of microcoils (a) infrared photogram (b) temperature distribution curve on line ac/bd.

Then we tested the rate of heating and cooling. The rapid rate of heating and cooling can ensure the reactants be in the right temperature field quickly, avoiding the failure of the reaction caused by other temperatures. In addition, the reaction time of the whole cycle can be reduced to improve the reaction efficiency. Figure 5(a) shows the heating rate at the current of 0.8A. The heating rate of the microchip rises up to 16 °C/s at the very beginning when the current loaded on the microcoils, indicating the rapid response of heating process. The average heating rate in the first 5 seconds is 6.8°C and relative high heating rate can last about 10s. Afterward, it rises slowly while the thermal expands and heats the ambient region. The infrared thermal images show detailed information of the thermal distribution as shown Fig. 5(b). The cooling of the micro-heater is also impressive, as demonstrated in Fig. 5(c) and 5(d). The highest cooling rate can be up to 15 °C/s, at very beginning when the power is off, and drops quickly in the subsequent 8 s. The results show that the PCR microfluidic chip has accurate temperature control ability and fast temperature response rate and laid a foundation to realize three-temperature cycle control.

Finally, according to the temperature conditions (95°C, 65°C, 72°C) required by the three reaction stages of common PCR reagents, the corresponding loading current was determined to be 0.63A - 0.45A - 0.50A based on the relationship between the stable temperature and current. As shown in Fig. 6(a), the square wave period of the square wave current signal is 3 min, and the loading time of each current section is 1 min. The curve of 10 cycles' temperature changing with current recorded by infrared thermographs is shown in Fig. 6(b). The difference between the stable temperature obtained within 1 min of each current flow and the preset temperature is less than 1°C. This proves that the cyclic control of the temperature field generated by the microcoils can be achieved by controlling the square wave current loading, with high temperature control accuracy and fast current response. We have also completed 40 cycles of temperature cycle experiments, and the temperature control is accurate and stable. The microfluidic chip can meet the requirements of temperature control accuracy and cycle times of the PCR process.

Optics EXPRESS

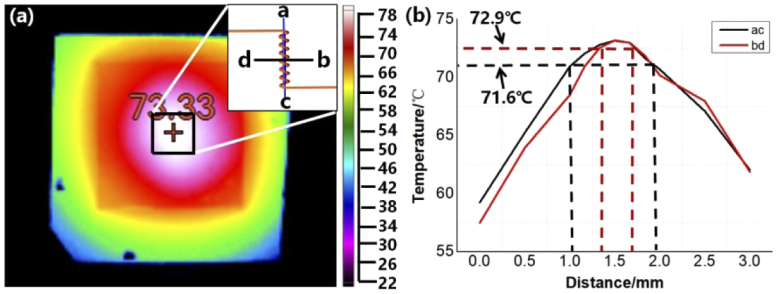


**Fig. 5.** (a) The heating rate in beginning 20s of heating period at the highest electric current of 0.8A. (c) The cooling rate in beginning 20s of cooling period. (b)(d) The infrared thermal image figures at different time.

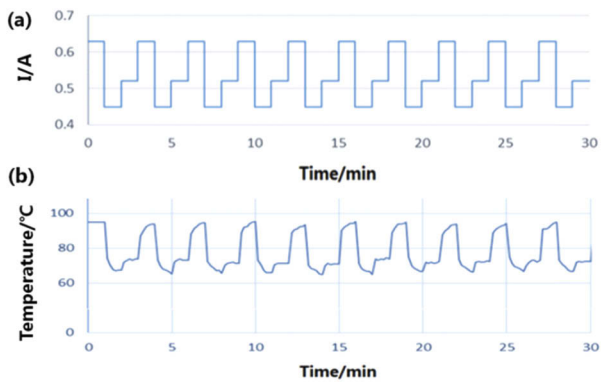


**Fig. 6.** Periodic variation of temperature with the periodic square electric current.

From the results of accuracy of temperature control, the rate of temperature heating/cooling and the cycle temperature test of the microfluidic chip, it can be seen that the microchip fabricated by the hybrid integrated method has accurate temperature control performance, rapid reaction rate and stable performance. It can meet the requirement of temperature field in PCR process. Therefore, the integrated microfluidic chip is expected to be applied to the core unit of small integrated PCR instrument.

## 4. Conclusions

In a summary, we presented 3D microfluidic chips integrated with microchannel and microcoils inside fused silica utilizing an enhanced femtosecond laser wet etching and liquid metal injection process. The experimental results demonstrated the capabilities of the device, including precise control of the temperature by the current, rapid heating and cooling process and stable performance, which can be used for PCR process. This technology could be used to fabricate various integrated micro-electronics, micro-sensors and microfluidics and pave a new avenue to develop next-generation 3D lab-on-chip (LOC) or MEMS devices.

## Funding

National Natural Science Foundation of China (61805192, 61875158, 61905188); National Key Research and Development Program of China (2017YFB1104700); China Postdoctoral Science Foundation (2019M653636).

Optics EXPRESS

## Acknowledgments

The International Joint Research Laboratory for Micro/Nano Manufacturing and Measurement Technologies; the Fundamental Research Funds for the Central Universities.

## Disclosures

The authors declare no conflicts of interest.

## References

1. R. Daw and J. Finkelstein, "Insight: Lab on a chip," Nature **442**(7101), 367 (2006).
2. G. M. Whitesides, "The origins and the future of microfluidics," Nature **442**(7101), 368–373 (2006).
3. S. Haeberle and R. Zengerle, "Microfluidic platforms for lab-on-a-chip applications," Lab Chip **7**(9), 1094–1110 (2007).
4. Z. Zou, X. Chen, Q. Jin, M. Yang, and J. Zhao, "A novel miniaturized PCR multi-reactor array fabricated using flip-chip bonding techniques," J. Micromech. Microeng. **15**(8), 1476–1481 (2005).
5. I. Sakellari, E. Kabouraki, D. Gray, V. Purlys, C. Fotakis, A. Pikulin, N. Bityurin, M. Vamvakaki, and M. Farsari, "Diffusion-Assisted High-Resolution Direct Femtosecond Laser Writing," ACS Nano **6**(3), 2302–2311 (2012).
6. E. Kabouraki, A. N. Giakoumaki, P. Danilevicius, D. Gray, M. Vamvakaki, and M. Farsari, "Redox Multiphoton Polymerization for 3D Nanofabrication," Nano Lett. **13**(8), 3831–3835 (2013).
7. Y. Hu, S. Rao, S. Wu, P. Wei, W. Qiu, D. Wu, B. Xu, J. Ni, L. Yang, J. Li, J. Chu, and K. Sugioka, "All-Glass 3D Optofluidic Microchip with Built-in Tunable Microlens Fabricated by Femtosecond Laser-Assisted Etching," Adv. Opt. Mater. **6**(9), 1701299 (2018).
8. H. Liu, F. Chen, Q. Yang, P. Qu, S. He, X. Wang, J. Si, and X. Hou, "Fabrication of bioinspired omnidirectional and gapless microlens array for wide field-of-view detections," Appl. Phys. Lett. **100**(13), 133701 (2012).
9. J. Choi, S. Rosset, M. Niklaus, J. R. Adleman, H. Shea, and D. Psaltis, "3-dimensional electrode patterning within a microfluidic channel using metal ion implantation," Lab Chip **10**(6), 783–788 (2010).
10. Y. Zhang, Y. Tian, H. Wang, Z. Ma, D. Han, L. Niu, Q. Chen, and H. Sun, "Dual-3D Femtosecond Laser Nanofabrication Enables Dynamic Actuation," ACS Nano **13**(4), 4041–4048 (2019).
11. D. Choudhury, W. T. Ramsay, R. Kiss, N. Willoughby, L. Paterson, and A. K. Kar, "A 3D mammalian cell separator biochip," Lab Chip **12**(5), 948–953 (2012).
12. Y. Liao, J. Song, E. Li, Y. Luo, Y. Shen, D. Chen, Y. Cheng, Z. Xu, K. Sugioka, and K. Midorikawa, "Rapid prototyping of three-dimensional microfluidic mixers in glass by femtosecond laser direct writing," Lab Chip **12**(4), 746–749 (2012).
13. D. Qian, L. Yang, Y. Zhang, C. Xin, Z. Hu, K. Hu, Y. Wang, D. Pan, J. Li, D. Wu, Y. Hu, and J. Chu, "Flexible and rapid fabrication of silver microheaters with spatial-modulated multifocal by femtosecond laser multiphoton reduction," Opt. Lett. **43**(21), 5335–5338 (2018).
14. D. Wu, S. Wu, J. Xu, L. Niu, K. Midorikawa, and K. Sugioka, "Hybrid femtosecond laser microfabrication to achieve true 3D glass/polymer composite biochips with multiscale features and high performance: the concept of ship-in-a-bottle biochip," Laser Photonics Rev. **8**(3), 458–467 (2014).
15. S. He, F. Chen, K. Liu, Q. Yang, H. Liu, H. Bian, X. Meng, C. Shan, J. Si, Y. Zhao, and X. Hou, "Fabrication of three-dimensional helical microchannels with arbitrary length and uniform diameter inside fused silica," Opt. Lett. **37**(18), 3825–3827 (2012).
16. C. Hnatovsky, R. S. Taylor, E. Simova, V. R. Bhardwaj, D. M. Rayner, and P. B. Corkum, "Polarization-selective etching in femtosecond laserassisted microfluidic channel fabrication in fused silica," Opt. Lett. **30**(14), 1867–1869 (2005).
17. F. Chen, C. Shan, K. Liu, Q. Yang, X. Meng, S. He, J. Si, F. Yun, and X. Hou, "Process for the fabrication of complex three-dimensional microcoils in fused silica," Opt. Lett. **38**(15), 2911–2914 (2013).
18. S. Jeong, J. Lim, M. Kim, J. Yeom, H. Cho, H. Lee, Y. Shin, and J. Lee, "Portable low-power thermal cycler with dual thin-film Pt heaters for a polymeric PCR chip," Biomed. Microdevices **20**(1), 14 (2018).
19. C. H. Wang, Y. Y. Chen, C. S. Liao, T. M. Hsieh, C. Luo, J. Wu, H. Lee, and G. Lee, "Circulating polymerase chain reaction chips utilizing multiple-membrane activation," J. Micromech. Microeng. **17**(2), 367–375 (2007).
20. K. T. L. Trinh and N. Y. Lee, "Glass-polytetrafluoroethylene-glass based sandwich microdevice for continuous-flow polymerase chain reaction and its application for fast identification of foodborne pathogens," Talanta **176**, 544–550 (2018).